Conference materials
UDC 544.536
DOI: https://doi.org/10.18721/JPM.153.333

Comparison of femtosecond laser, hydrothermal and microwave synthesis of fluorescent products from L-lysine

A. A. Astafiev [1]✉, A. M. Shakhov [1], M. S. Syrchina [1], D. V. Shepel [1], V. A. Nadtochenko [1]

[1] N. N. Semenov Federal Research Center of Chemical Physics of the Russian Academy of Sciences, Moscow, Russia

✉ astafiev.artyom@gmail.com

Abstract. Femtosecond laser synthesis of fluorescent products from essential amino acids in living cells and tissues can be exploited in fluorescent bioimaging. To gain insight into reaction mechanism and a role of thermal processes we examine synthesis of fluorescent products from L-lysine by femtosecond laser irradiation, hydrothermal and microwave synthesis and perform comparative analysis of reaction products. Our results indicate that compared with purely thermal synthetic routes femtosecond laser synthesis favours formation of carbon dots-type fluorescent nanomaterials.

Keywords: femtosecond laser pulses, nonlinear absorption, laser treatment, nanomaterials, luminescent carbon dots, photobleaching, photostability

Funding: This study was funded by Russian Scientific Foundation grant No. 21-72-20169. The measurements were performed in the FRCCP shared research facilities No. 506694 and large-scale research facilities No. 1440743.

Citation: Astafiev A. A., Shakhov A. M., Syrchina M. S., Shepel D. V., Nadtochenko V. A., Comparison of femtosecond laser, hydrothermal and microwave synthesis of fluorescent products from L-lysine. St. Petersburg State Polytechnical University Journal. Physics and Mathematics, 15 (3.3) (2022) 171–176. DOI: https://doi.org/10.18721/JPM.153.333

Материалы конференции
УДК 544.536
DOI: https://doi.org/10.18721/JPM.153.333

Сравнение лазерного фемтосекундного, гидротермального и микроволнового синтеза флуоресцентных продуктов из L-лизина

А. А. Астафьев [1]✉, А. М. Шахов [1], М. С. Сырчина [1], Д. В. Шепель [1], В. А. Надточенко [1]

[1] Федеральный исследовательский центр химической физики им. Н. Н. Семенова Российской Академии Наук, Москва, Россия

✉ astafiev.artyom@gmail.com

Аннотация. В настоящей работе проведен сравнительный анализ механизмов получения люминисцентных углеродных точек, а также основных физико-химических характеристик продуктов, полученных в результате трех различных методов синтеза – лазерного фемтосекундного, микроволнового и гидротермального.

Ключевые слова: фемтосекундные лазерные импульсы, нелинейное поглощение света, лазерная модификация материалов, наноматериалы, люминесцентные углеродные точки, фотовыцветание, фотостабильность

Финансирование: Работа выполнена при финансовой поддержке РНФ, грант № 21-72-20169. Измерения были выполнены в центре коллективного пользования № 506694 и на уникальной научной установке № 1440743.

Ссылка при цитировании: Астафьев А. А., Шахов А. М., Сырчина М. С., Шепель Д. В., Надточенко В. А., Сравнение лазерного фемтосекундного, гидротермального и микроволнового синтеза флуоресцентных продуктов из L-лизина // Научно-технические ведомости СПбГПУ. Физико-математические науки. 2022. Т. 15. № 3.3. С. 171–176. DOI: https://doi.org/10.18721/JPM.153.333

Introduction

Production of fluorescent species from biomolecules in living cells and tissues in situ by femtosecond laser irradiation offers many unique advantages in fluorescent bioimaging [1–2]. We demonstrated that femtosecond laser synthesis of fluorescent carbon dots from essential amino acid L-lysine provides a potential route of fluorescent species formation in living cells [3]. Laser-induced heating can be one of mechanisms responsible for carbon dots synthesis and fluorescent carbon dots can be also produced from amino acids, including L-lysine, by a more conventional thermal-driven reactions using solvothermal or microwave synthesis [4, 5]. In order to gain a better understanding of the role of thermal mechanisms and peculiarities of femtosecond laser synthesis we analysed optical properties, morphology and chemical composition of products obtained from L-lysine aqueous solution by three different routines: femtosecond laser, hydrothermal and microwave synthesis (hereafter samples Lys-FS, Lys-HT and Lys-MW respectively).

Materials and Methods

1. Synthesis and purification of products.

Lys-FS: 2 ml of L-lysine aqueous solution (0.1 g/mL) in a quartz cuvette was irradiated with trains of femtosecond laser pulses focused by a spherical lens (f = 8 mm, 0.5NA). Central wavelength of laser pulses was 800 nm, repetition rate – 1 kHz, duration – 50 fs, pulse energy – 1.4 mJ. Lys-HT: 10 ml of 0.5 g/mL L-lysine solution in a PTFE container was heated in an oven for 30 hours at 220 °C. Lys-MW: 5 ml of 0.1 g/mL L-lysine solution in a glass vial was heated in a domestic microwave oven for 1 min at 800 W. In order to remove unreacted L-lysine the samples were dialyzed for 72 hours in 2,000 MWCO dialysis units.

2. Samples characterization.

UV-Vis absorption and photoluminescence spectra of aqueous solutions of the samples in a 3.5-ml quartz cuvette were recorded with Shimadzu UV-3600 spectrophotometer and Shimadzu RF-5031PC spectrofluorometer. Fluorescence quantum yield at 356 nm excitation wavelength was estimated with the slope method using ethanol solution of anthracene ($\Phi = 0.27$) as a reference sample. Fluorescence decay curves of samples aqueous solutions were recorded at 450 nm emission wavelength by the a Beckr-Hickl SPC-150N time-correlated single photon counting system using excitation with laser pulses of the femtosecond laser oscillator (Tsunami, Spectra-Physics) with 360 nm central wavelength and 60 MHz repetition rate. For measurement of fluorescence anisotropy decay we recorded two fluorescence decay curves for emission with polarization parallel and perpendicular to the excitation laser and calculated emission anisotropy as a function of time.

Samples diluted in ethanol and dried on a cover slip were analyzed with an atomic-force microscopy (AFM) unit (SMENA-B, NT MDT) in an intermittent contact mode. High resolution transmission electron microscopy (HRTEM) images were recorded on a JEM 2100F high-resolution transmission electron microscope (JEOL Co. Ltd., Japan). Infrared absorption spectra were collected using a Bruker Lumos II FTIR microscope-spectrometer in a reflection mode from drops the samples aqueous solutions dried on the surface of Ag mirror. Raman spectra were collected with a Bruker Senterra Raman microscope-spectrometer using gold nanoparticles photocatalytically grown from HAuCl4 aqueous solution for surface enhancement of the Raman scattering signal. Elemental analysis with energy-dispersive (EDS) X-ray spectroscopy was performed using a Prisma-E electron microscope (Thermo-Fisher), using L-lysine with a known C:N:O ratio (3:1:1) as a calibration sample.

Results and Discussion

Originally colorless L-lysine aqueous solution became dark red or black after laser, hydrothermal or microwave treatment and exhibited strong blue fluorescence, which indicated formation of colored and luminescent products from L-lysine. After dialysis versus a 2,000 MWCO dialysis membrane **Lys-FS** solution retained most (55%) of original integral UV-Vis absorption, whereas **Lys-HT** and **Lys-MW** retained only 5.5 and 8% of integral absorption respectively. This result suggests that hydrothermal or microwave treatment of L-lysine mostly resulted in formation of colored products with small molecular weight, which could pass through pores of the dialysis membrane. At the same time Lys-FS contained nanosized particles which were retained by the membrane. Presence of nanosized products in Lys-FS was confirmed by AFM and HRTEM images which visualized irregular-shaped nanoparticles with characteristic sizes in the range from nanometers to ca. 10–20 nanometers (Fig. 1). Also HRTEM images of the nanoparticles revealed onion-type structure consisting of concentric layers with the interlayer distance of ca. 0.35 nm (Fig. 1, *b*). This distance almost coincides with the graphite [002] lattice fringe (0.335 nm), suggesting that these nanoparticles were so-called carbon onions, consisting of concentric fullerene-type shells [6].

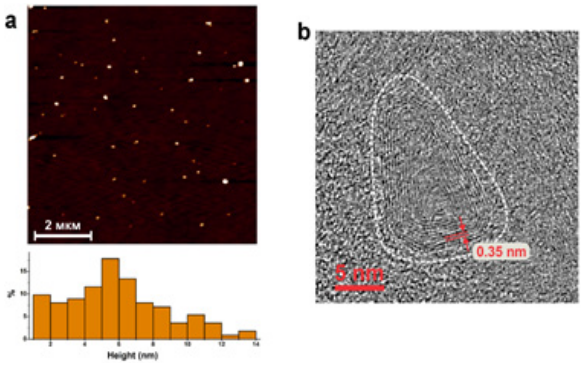

Fig. 1. AFM image of Lys-FS naoparticles on a glass substrate and their height distribution (*a*); HRTEM image of a single Lys-FS nanoparticle (*b*)

FTIR reflectance spectra of all the purified samples exhibited characteristic secondary amide bands at ca. 1650–1650, 1550 and 1300 cm^{-1} (Fig. 2, *a*), indicative of peptide bonds formation. Thus products of the thermal or laser treatment contained peptide chains formed by polycondensation of L-lysine molecules. Second derivative analysis reveals position of Lys-FS amide I and amide III bands at 1547 and 1302 cm^{-1}, which is indicative of the α-helix peptide conformation [7, 8]. At the same time in Lys-HT the position of amide I (1666 cm^{-1}) and amide III (1311 cm^{-1}) show a more disordered secondary structure consisting of a combination of extended P_{II} helix and turns. Additionally FTIR spectra exhibited CH_2 stretching and bending vibrations from the lysine side chains, COO- stretching vibrations from peptide terminal residues, NH, OH and CH stretching vibrations.

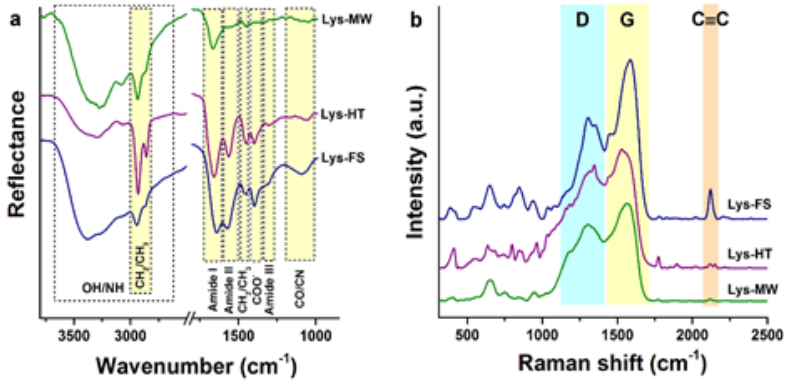

Fig. 2. FTIR (*a*) and Raman (*b*) spectra of **Lys-FS**, **Lys-HT** and **Lys-MW**

Raman spectra of all the three samples demonstrated broad bands centered at 1310 and 1580 cm^{-1}, which are D and G bands typical for carbonaceous materials and are indicative of sp^2-hybridized carbon forming C = C bonds and honeycomb structures of fused benzene rings. Another band at 2120 cm^{-1} attributed to C ≡ C stretching was especially strong in Lys-FS spectra. Thus, in addition to the peptide chains with sp^3-hybridizedcarbon all the samples contained unsaturated fragment with sp^2 and sp^3-hybridized carbon.

Polycondensation of L-lysine molecules into peptide chains removes one oxygen atom from each residue and therefore must result in decrease of O and increase of C and N elemental content compared with L-lysine. EDS measurements for Lys-HT confirm these changes and show that its elemental content was similar to poly-lysine (Table 1), thus it mostly consists of lysine olygormers (polymers). At the same time Lys-FS and Lys-MW exhibited much larger oxygen content than poly-lysine, probably due to oxidation in presence of the atmospheric air, which compensated for a loss of oxygen in the polycondensation reaction. This oxidation is confirmed by a stronger OH stretching band on the FTIR spectra of Lys-FS and Lys-MW compared with Lys-HT. C:N atomic ratio for all the three samples was larger than 3:1 ratio expected for L-lysine or poly-L-lysine. This change is indicative of the onset of carbonization and removal of nitrogen. The C:N ratio and consequently the scale of carbonization was the largest for Lys-FS.

Table 1

CNO Elemental composition of the samples compared with L-lysine and poly-lysine

Sample	C (at. %)	N (at. %)	O (at. %)	C:N ratio	N:O ratio
L-lysine	60	20	20	3	1
Poly-L-lysine	66.7	22.2	11.1	3	2
Lys-FS	61.1	17.8	21.2	3.43	0.84
Lys-HT	65.5	20.8	13.7	3.15	1.52
Lys-MW	61.2	20.0	18.8	3.06	1.06

In summary, the chemical analysis revealed that products of L-lysine heating or laser treatment are formed by processes of L-lysine polycondensation, oxidation and partial carbonization of resulting poly-(olygo-)peptides. Carbonization converts peptide fragments to unsaturated moieties with sp^2- and sp^3-hybridized carbon, which is a probable mechanism for formation of light-absorbing chromophore groups. Whereas hydrothermal and microwave treatment mostly produces relatively short L-lysine olygomers, femtosecond laser treatment tends to produce larger polymer nanoparticles and induces larger oxidation and carbonization effect. Carbonization and graphitization of polymer nanoparticles can produce carbon onion structures revealed by the HRTEM.

All the three samples had strong absorption with absorption peaks and shoulders in the ultraviolet range, whereas their visible absorption was relatively weak and structureless (Fig. 3). Presence of near-UV and visible absorption demonstrates effective formation of chromophores with conjugated systems from L-lysine. All the samples exhibited strong photoluminescence with emission maxima in the blue range (at 430–440 nm) and excitation maxima near 350 nm (Table 2). Excitation maxima did not coincide with peaks and shoulders on the absorption spectrum, indicating that most UV-absorbing chromophores were nonfluorescent.

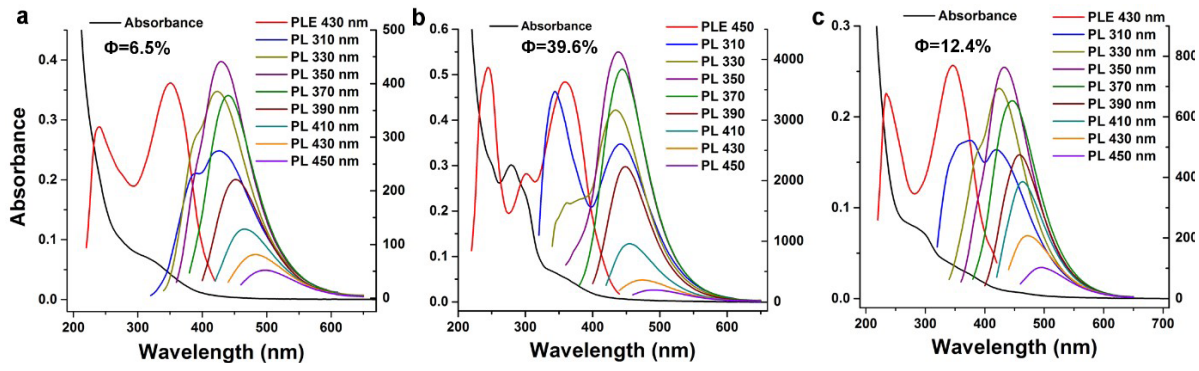

Fig. 3. UV-Vis absorbance, photoluminescence emission (PL) and excitation (PLE) spectra of Lys-FS (*a*), Lys-HT (*b*) and Lys-MW (*c*) in aqueous solution. Φ – fluorescence quantum yield.

Visible photoluminescence was excitation-dependent: its emission peak shifted to longer wavelengths with increase of the excitation wavelength. The large shift (from ca. 430 to 500 nm for Lys-FS) suggests a multicomponent emission from several blue- and green-emitting fluorescent chromophores. The shift of the emission maximum was accompanied by attenuation of the emission intensity corresponding to excitation of green-emitting instead of blue-emitting chromophores. This attenuation, expressed as I_{450}/I_{350} ratio in the Table 2 was the smallest and the spectral shift was the largest for the Lys-FS demonstrating that the laser-treated L-lysine had the largest population of green-emitting chromophores.

Table 2

Principal photoluminescence parameters of aqueous solutions of Lys-FS, Lys-HT and Lys-MW. Em.Max and Ex.Max – emission and excitation maximum wavelength, Φ – fluorescence quantum yield, Trot – fluorescence anisotropy decay time (rotation time), I_{450}/I_{350} – ratio of integral luminescence intensity excited at 450 and 350 nm

Sample	Em.Max. (nm)	Ex.Max (nm)	Φ (%)	Lifetime (ns)	T_{rot} (ns)	I_{450}/I_{350}
Lys-FS	429	341	6.5	1.73	1.39	0.150
Lys-HT	439	359	39.6	5.19	0.37	0.046
Lys-MW	433	346	12.4	1.60	0.26	0.119

In accordance with its higher quantum yield Lys-HT demonstrated larger fluorescence lifetime, while similar decay kinetics and lifetimes of Lys-FS and Lys-MW suggests that they comprise similar chromophore groups. A large anisotropy decay time of Lys-FS corresponding to a hydrodynamic volume of 5.7 nm^3 indicates that its luminescent chromophores are embedded in slowly rotating rigid nanosized poly-lysine particles. At the same time chromophore groups of Lys-HT and Lys-MW are evidently attached to shorter (and probably flexible) peptide chains, leading to their faster rotation in solution.

Conclusion

Thermal treatment of L-lysine aqueous solution under hydrothermal, microwave or femtosecond laser irradiation conditions yields products with visible absorption and bright excitation-dependent visible fluorescence. Fluorescence characteristics depend on the synthesis method and femtosecond synthesis produced products with stronger green emission. Chemical transformation of L-lysine includes polycondensation, oxidation and carbonization and results in formation of a combination of lysine olygomers (polymers) and unsaturated chromophore groups. Femtosecond laser exposure yields luminescent nanoparticles (carbon dots), which are highly oxidized and carbonized, frequently exhibit carbon onion structure and have a large content of triple C ≡ C bond. Our results confirm that luminescent species can be formed from amino acids and peptides in material of cells and tissues under pulsed laser irradiation and shed light on their formation mechanism.

REFERENCES

1. **Sun Q., Qin Z., Wu W., Lin Y., Chen C., He S., Li X., Wu Z., Luo Y., Qu J.,** In vivo imaging-guided microsurgery based on femtosecond laser produced new fluorescent compounds in biological tissues, Biomedical Optics Express. 9 (2018) 581–590.

2. **Astafiev A. A., Shakhov A. M., Osychenko A. A., Syrchina M. S., Karmenyan A. V., Tochilo U. A., Nadtochenko V. A.,** Probing intracellular dynamics using fluorescent carbon dots produced by femtosecond laser in situ, ACS Omega. 5 (21) (2020) 12527–12538.

3. **Astafiev A. A., Shakhov A. M., Gulin A. A., Vasin A. A., Gubina M. V., Syrchina M. S., Nadtochenko V. A.,** Femtosecond laser synthesis and comparative analysis of fluorescent carbon dots from L-lysine aqueous solution, Journal of Physics: Conference Series. 2086 (2021) 012121.

4. **Sahiner N., Suner S. S., Sahiner M.,** Nitrogen and Sulfur Doped Carbon Dots from Amino Acids for Potential Biomedical Applications. Journal of Fluorescence, 29 (2019) 1191–1200.

5. **Bartelmess J., Giordani S.,** Carbon nano-onions (multi-layer fullerenes): chemistry and applications, Beilstein Journal of Nanotechnology, 5 (2014) 1980–1998.

6. **Yang J., Chen W., Liu X., Zhang Y., Bai Y.,** Hydrothermal synthesis and photoluminescent mechanistic investigation of highly fluorescent nitrogen doped carbon dots from amino acids, Materials Research Bulletin. 89 (2017) 26–32.

7. **Mirtič A., Grdadolnik J.,** The structure of poly-l-lysine in different solvents, Biophysical Chemistry.175–176 (2013) 47–53

8. **Grdadolnik J., Mohacek-Grosev V., Baldwin R. L., Avbelj, F.,** Populations of the three major backbone conformations in 19 amino acid dipeptides, Proceedings of the National Academy of Sciences. 108 (5) (2011) 1794–1798.

THE AUTHORS

ASTAFIEV Artyom A.
astafiev.artyom@gmail.com
ORCID: 0000-0001-9269-414X

SHEPEL Denis V.
d.shepel@technoinfo.ru
ORCID: 0000-0003-2437-7219

SHAKHOV Aleksander M.
physics2007@yandex.ru
ORCID: 0000-0002-0958-2903

NADTOCHENKO Victor A.
nadtochenko@gmail.com
ORCID: 0000-0002-6645-692X

SYRCHINA Maria S.
wrongclue@gmail.com
ORCID: 0000-0002-5318-8903

Received 18.07.2022. Approved after reviewing 20.07.2022. Accepted 09.09.2022.